

HIRDS.V3: High Intensity Rainfall Design System – The method underpinning the development of regional frequency analysis of extreme rainfalls for New Zealand

Craig Thompson
25 February 2010
Revision 1 – 11 March 2011

Introduction

“Extreme value theory provides a solid theoretical basis and framework for extrapolation”, Laurens de Haan & Ana Ferreira, 2006

The statistics of extremes play a vital role in engineering practice for water resource management and design (Katz et al., 2002). From the perspective of mitigation and protection of infrastructure and human life from flooding, much scientific attention is given to the estimation of hydro-meteorological extremes. While storm frequency assessments, based on flood data are to be preferred, the analysis of rainfall data is often more convenient due to the larger networks, often with longer records, and potentially more easily transferable from site to site. However, at some sites there can be limited data available on extremes and fitting an extreme value distribution can lead to difficulties, particularly in the estimation of extreme quantiles (Ailliot et al., 2009). As is often the case, within a suitably defined “region”, data from several sites show similar extreme-statistical properties, and can be combined to provide more accurate event quantile estimates (Hosking and Wallis, 1997). In this context, a region can correspond to a fixed geographic area, or it can refer to a grouping or collections of sites (Stewart et al., 1999) of the same environmental variable.

For more than three decades, regional frequency analyses of extreme rainfalls and floods have been undertaken in New Zealand (Tomlinson, 1980; Thompson, 1992, 2002 [for rainfall]; Beable and McKerchar, 1982; McKerchar and Pearson, 1989 [for floods]). A computer-based procedure for estimating rainfall event quantiles, called HIRDS (High Intensity Rainfall Design System), was first developed in 1992 and was based on Tomlinson’s graphical method of rainfall frequency analysis. In 2002, the calculation of high intensity rainfalls were revised and updated to incorporate a large increase in archived rainfall data, and to take advantage of the robust analysis techniques afforded by regional frequency analysis. The underlying method in the second version of HIRDS (Thompson, 2002) is an *index-frequency* procedure. The *index-variable* is a relatively common event (Dalrymple, 1960; Stewart et al., 1999), such as the *median annual maximum rainfall* that can be computed typically from the available record. The *frequency-variable* is derived from a regional analysis where data from several sites are combined to estimate a dimensionless *rainfall growth curve*, and represents a set of factors at different recurrence intervals relative to the index variable.

Estimates of high intensity rainfall for New Zealand have been further revised and updated. This paper details the methods and techniques used in the third version of HIRDS. A web-based application (<http://hirds.niwa.co.nz>) provides high intensity rainfall tables for New Zealand and will allow users the ability to download tables directly to their PC.

Data

Monthly maximum rainfall¹ records for standard durations from 10 minutes to 72 hours, were obtained from three principal sources: NIWA's nationally significant data bases – Climate Database (data to end 2008) and Water Resources Archive (end 2005), and from New Zealand Regional Council archives (end 2005). A total of 3213 sites were available for further analysis, with the majority (2177) being manual rain gauges read once daily at 9am and covering the period of 1 to 3 days. The fixed duration raingauge data were converted to equivalent 24, 48, and 72-hour values (i.e. unconstrained to end at 9am) using adjustment factors (Coulter and Hessel (1980); Tomlinson (1980)) of 1.14, 1.07 and 1.04 respectively. These factors are in agreement to those given WMO (1983).

Precipitation exhibits large fluctuations in both time and space (see for example Austin and Houze, 1970); yet in spite of this near neighbour rainfalls tend to show high inter-site correlations (Nandakumar et al, 1997). Rainfall sites within 500 m of each other were merged into composite site series. This allowed the extension of the high intensity time series if they were mutually exclusive. Where rainfall records overlapped, the maximum value of the contributing sites was chosen for the extreme rainfall series. This process also provided an estimate of the extreme if missing values existed within any of the series. Amalgamation reduced the total number of sites to 2697.

Annual maximum rainfall series at each site were created from the monthly maximum series if each annual maximum came from a year with at least 10 months of record, and if there were at least 6-years of annual values in each series. In the subsequent index-frequency analysis, the influence of the shorter rainfall series is small when compared to the longer ones. Outliers in the annual maximum series were retained, as they tend to have only a small effect on the estimation of quantiles if efficient parameter estimation methods such as maximum likelihood or L-moments are used to fit extreme value distributions (Cunane, 1989).

Although it is common to have larger data sets for single-site analyses in order to provide reasonably robust estimates, using a minimum of 6-years in a regional frequency analysis, means that the influence of short records will be small when compared to the longer ones.

¹ Monthly maximum rainfall comprises the largest rainfall within the specified duration in each calendar month.

Regional frequency analysis

A fundamental issue in the estimation of quantiles is the need to extrapolate to recurrence intervals significantly larger than the available records. This can be solved using regionalization, a standard practice for improving the estimation of event quantiles at sites with comparatively short records. Among the various regionalization procedures, a widely used one is *the index-flood* (also called index-rainfall or index-frequency) method first proposed by Dalrymple (1960) for flood frequency estimation. The basic principle of this approach is defining statistically homogeneous regions containing sites with similar frequency distributions apart from a scaling factor (the index variable). Dalrymple defined the index-variable as the mean annual flood (i.e. the 2.33-year recurrence interval derived from the frequency curve for each site), and the regional growth curve (frequency-variable) from the median of at-site event quantiles estimated from empirical at-site growth curves. Mathematically, for m sites in a region, the q^{th} event quantile at site j is: $x_j(q) = \mu_j \xi(q)$, where μ_j is the index-rainfall for site j , ξ_j is the regional q^{th} quantile, and the quantile q is the cumulative probability of the underlying frequency distribution.

Index-Frequency Method: Rainfall index variable

Estimating the median annual maximum

In this report, and in line with other studies, (Faulkner, 1999, Stewart et al., 1999, Jakob et al., 2005, Thompson 2002) the median annual maximum rainfall, R_{med} , was used in preference to the mean annual maximum rainfall. The median has an annual exceedance probability (equivalent to $1 - q$) of 0.5, corresponding to an annual recurrence interval of 2-years and is expected to be exceeded “every other year”. More importantly, it is a robust and resistant estimator of location, and is not usually affected by the skewness of the distribution or by the presence of outliers. It is a relatively common event that is usually computed from the at-site records.

Robson and Reed (1999) provide complimentary procedures in computing the index-rainfall based on the record length of the available at-site data. For series with at least 14 years of ranked annual maxima, the median annual maximum is the middle-ranking value or 50th percentile. When the record length is shorter data are extracted in a peaks-over-threshold form, and an annual exceedance series is created containing on average one event per year. In general peaks-over-threshold can provide improved estimates of event quantiles, as the procedure utilizes multiple rainfall exceedances in a year that would otherwise not be included if there were just annual maxima. Robson and Reed provide the theoretical link between peaks-over-threshold and annual maximum series. R_{med} is evaluated by finding a rainfall for which the annual exceedance probability is 0.5.

A variation of the Robson and Reed scheme was applied in this study. At sites of 6 – 20 years of records, the median annual maximum is determined from ranked monthly maxima using a peaks-over-threshold method, while at sites with longer records (more than 20 years), the 50th percentile of ranked annual maxima were computed. Figure 1 shows a scatter-plot of the index rainfall computed by the two methods. On the y-axis of the median from the annual maximum series, and on the x-axis are the median from the equivalent peaks-over-threshold approach. There is very close agreement. Points with greatest departure from equality line tend to be sites with relatively short records.

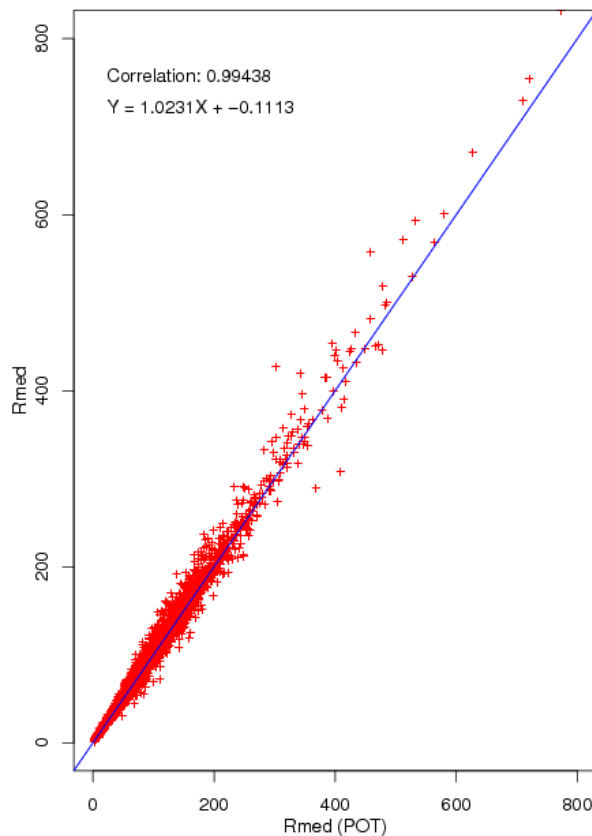


Figure 1. Scatter-plot of median annual maximum rainfall. On the y-axis are medians (R_{med}) obtained from the 50th percentile of annual maximum rainfalls, and on the x-axis the medians ($R_{med(POT)}$) are computed from a peaks-over-threshold method of monthly maxima (after Robson and Reed, 1999). The solid line is the equality $R_{med} = R_{med(POT)}$

Uncertainty in median annual maximum rainfall

The approximate variance of the median annual maximum rainfall, R_{med} , is given by Kendall and Stuart (1977) as $Var(X) \approx \frac{1}{4Nf^2(x)}$, where N is the sample size and f is the probability distribution function of the underlying frequency

distribution. For a Generalised Extreme Value distribution this becomes $\frac{\alpha^2}{N}(\log 2)^{2k-2}$ (Ailliot et al, 2009), where α and k are the scale and shape parameters of the distribution. As no assumption has been made on the underlying frequency distribution for R_{med} , resampling methods (Robson and Reed, 1999) are used to estimate the uncertainty (or standard errors) associated with the median annual maximum rainfall. For large sample sizes a *balanced resampling* method is used, and for small record lengths, a *factorial standard error* approach is used.

The basic idea of resampling is to take the observed data set and generate hypothetical samples (Reed, 1999). In balanced resampling, the observed data values are replicated M times to form a super-sample data set. These values are randomly re-ordered and divided into M sets of data. The median of each resample is derived from which the standard error is computed.

The factorial standard error, *fse*, is the exponential of the standard error on a logged scale, and is used to estimate the uncertainty in R_{med} in terms of multiplicative errors (Robson and Reed, 1999). Empirically derived factorial standard errors from New Zealand data sets are given in Table 1. Values close to 1 indicate good estimates of the median annual maxima.

Table 1. Factorial standard errors for New Zealand using annual maximum rainfall series

N	6	8	10	12	14	16	18	20	30
fse	1.143	1.127	1.105	1.093	1.084	1.075	1.069	1.062	1.038

The standard error is approximated by the 68 percent confidence interval ($R_{med}/fse, R_{med}*fse$) (Reed, 1999, Robson and Reed, 1999), and since the standard error estimate is symmetric about R_{med} , then the uncertainty associated with the median annual maximum is $se \approx R_{med}(fse - 1)$.

Based on the analysis methods of the previous paragraph a linear relationship between the logarithms of the variance and median annual maximum (Figure 2) exists, one that is largely independent of sample size. Variances increase monotonically as medians increase. An empirical relation for uncertainty in R_{med} is given by $se = 0.107R_{med}^{0.946}$, and is similar to the one found for the earlier version of HIRDS (Thompson, 2002).

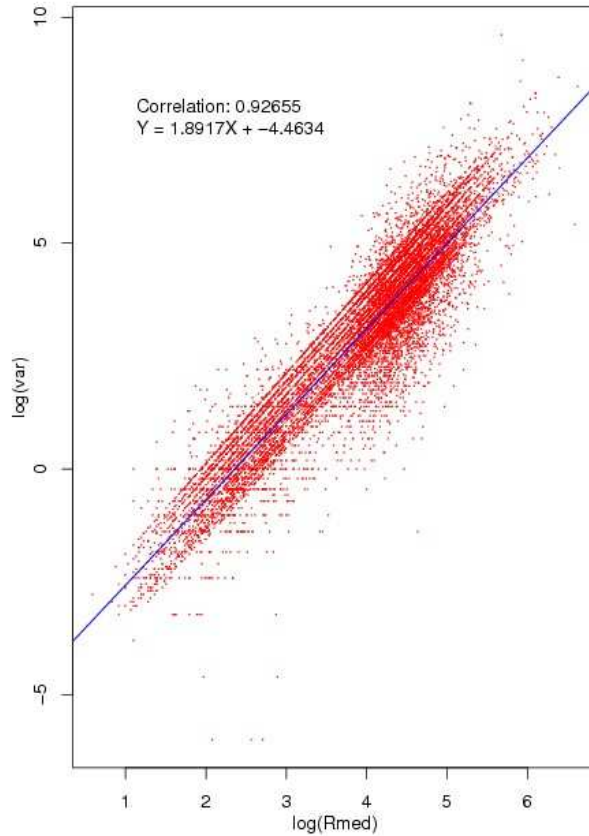


Figure 2. Relationship between the logarithm of the variance of median annual maximum rainfall and the logarithm of median annual maximum rainfall.

Mapping the median annual maximum rainfall

Computing design rainfalls with regional frequency analysis methods involves mapping the median annual maximum rainfall as well as parameters of the regional growth curves. Mapping the median rainfall involved fitting thin-plate smoothing splines as implemented by ANUSPLIN (Hutchinson, 1995, 2000). The spline is a surface that is fitted to spatially distributed data with some error assumed at each data point, so that the surface can be smoother than if the data fitted exactly. The thin-plate smoothing spline for n data values at site x_i (Hutchinson and Gessler, 1994) is

$$z(x_i) = f(x_i) + \varepsilon(x_i) \quad i = 1, \dots, n$$

where $f(x_i)$ is an unknown smooth function to be estimated from the observations $z(x_i)$ (i.e. the median annual maximum rainfall), ε_i are the zero mean random errors with a common variance σ^2 .

The function $f(x_i)$ is estimated by minimising

$$\sum_{i=1}^n [z(x_i) - f(x_i)]^2 + \lambda J_m(f)$$

where $J_m(f)$ is a roughness penalty of the spline function f , defined in terms of m^{th} order partial derivatives and λ is the smoothing parameter. The value of the smoothing parameter is a compromise between the roughness of the surface and closeness of fit to the data. It is often determined by the method of generalised cross validation (GCV) (Hutchinson, 1995, 2000) in which each site is omitted in turn from the estimation of the fitted surface. This is repeated for a range of smoothing parameter values and the value that minimises the predictive error is selected to give the optimum smoothing. However in many hydro-meteorological data sets, which have few data and are often noisy, using the GCV criterion can result in unrealistically smooth maps with unacceptably large differences between the data and spline surface. To address this Zheng and Basher (1995) manipulated the signal to error properties of the data and spline fit and found that enforcing a global signal to error ratio (a diagnostic measure available from the spline fitting process) provides a useful and intuitive procedure for understanding and controlling the fitting. The larger the signal to error ratio is, the closer the fitted surface passes through the data, and the smaller the error of the fitted values, although robust spline fits in data sparse areas are more likely when the ratio is no more than one (Hutchinson and Gessler, 1994). However, the final selection of the ratio is usually left to user, to allow for their expertise and prior knowledge of the characteristics of the data being fitted.

Surfaces of median annual maximum rainfall were fitted with a tri-variate thin-plate spline, with the three independent variables being longitude, latitude and elevation above sea level. The tri-variate spline of rainfall allows for a continuous spatially varying dependence on elevation (Hutchinson 1995), is well suited to applications over complex terrain as is found in New Zealand, and can provide a robust method of surface fitting meteorological data from moderately sparse data networks. Correctly specifying elevation units is critical to the performance of thin-plate splines (Hutchinson, 1995); as a rule the elevation scaling should be 100 times the horizontal scale. With position coordinates of latitude and longitude, elevation should be in kilometres.

All 10 surfaces were fitted using a common signal to error ratio of 2.5 and were mapped with ANUSPLIN onto a 2km by 2km digital elevation model. Fitting multiple surfaces simultaneously (i.e. 10 minutes to 12 hours, and 24 to 72 hours) ensures consistency between the surfaces in the group. For 10 minutes to 12 hours there were 806 sites available to be fitted, and for the other three durations around 2630 sites. Maps showing the one and 24 hour median annual maximum rainfall over New Zealand are given in Figures 2 and 3. The strong influence of New Zealand's orography on the rainfall pattern is noticeable in that the largest values are found in the mountainous regions of both islands.

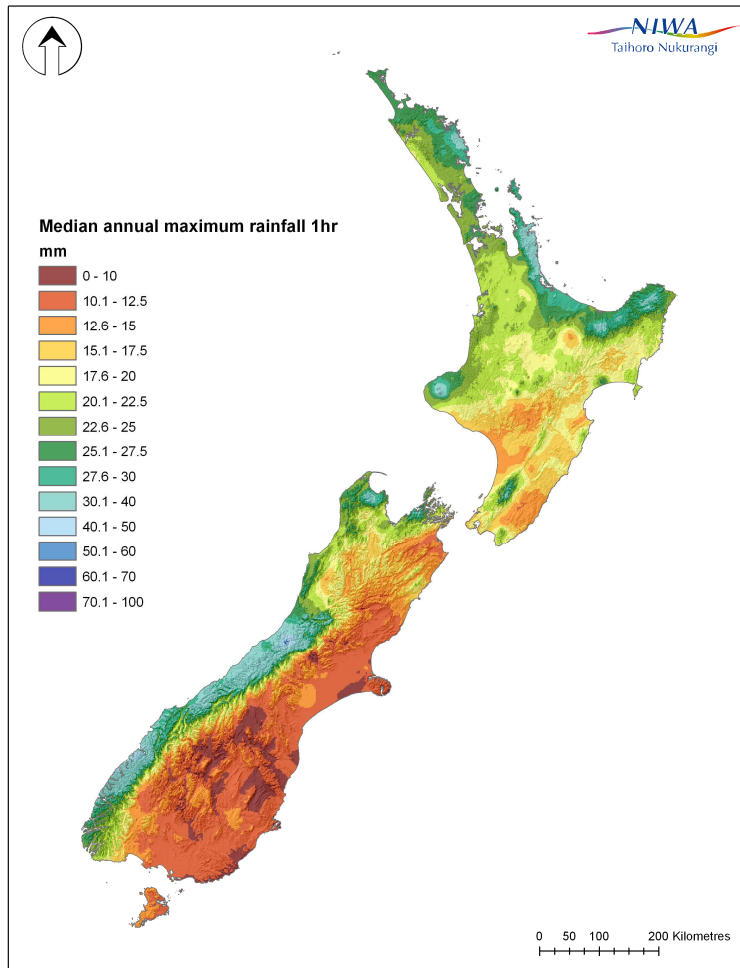


Figure 2. Index- rainfall variable: Median annual maximum rainfall for 1-hour duration.

Standard errors of the fitted spline surfaces are provided by ANUSPLIN. Hutchinson (1998) found interpolation errors decreased by about 10 percent if rainfall data are transformed before the spline surface is fitted, a finding also confirmed by Tait et al, (2006). For a square-root transformation, the standard error is positively correlated with rainfall and is given by

$$se(X^2) = 2s(X^2 + s^2 / 2)^{0.5}$$

where X is the transformed median annual maximum rainfall, and s is the prediction standard error computed from the error covariance matrix of the spline coefficients. Standard error maps are useful in identifying which sites have the largest uncertainty associated with their expected value: it is often found in data sparse regions. The uncertainty calculation is the standard error associated in fitting the spline surface to the data, and is not the level of uncertainty associated with the median annual maximum.

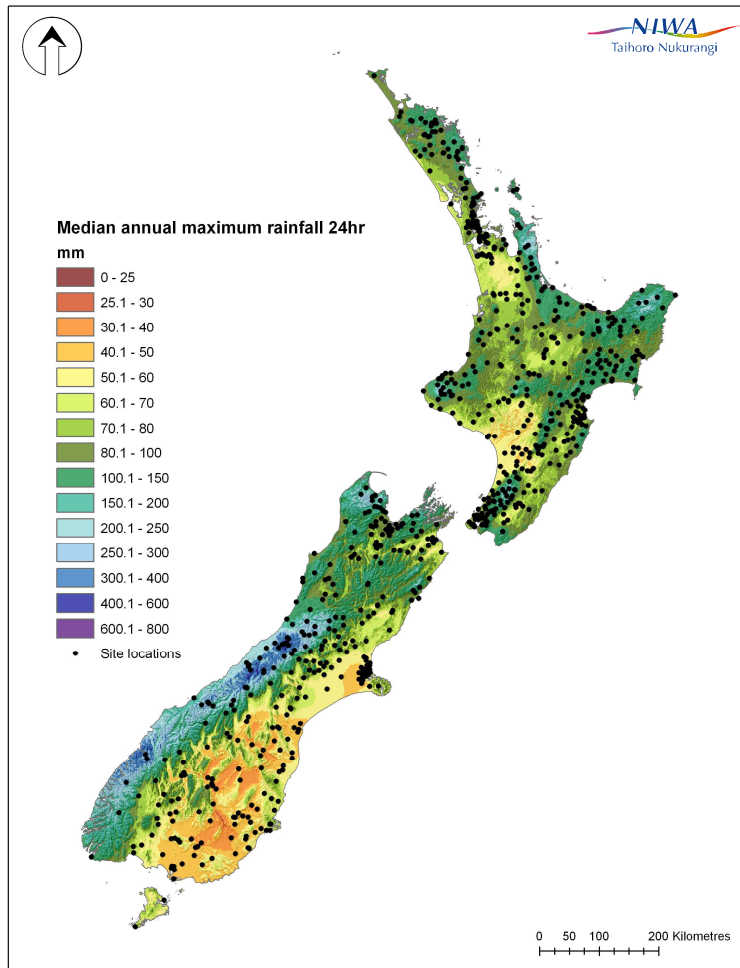


Figure 3. Index-rainfall variable: Median annual maximum rainfall for 24-hour duration.

Index-Frequency Method: Frequency variable and regional growth curves

The second component in the index-frequency method is the development and application of regional growth curves derived from cumulative frequency distributions of fitted annual maximum rainfalls. The following section describes the procedures in selecting, fitting and mapping an appropriate extreme-value distribution; in forming homogeneous regions from which growth curves can be derived.

Selection of frequency distribution

The Generalised Extreme Value (GEV) distribution (Jenkinson, 1955) was selected to fit annual maximum rainfalls in New Zealand for the 10 standard storm durations. The choice of the GEV was chosen on the basis of fitting frequency distributions (GEV, Gumbel [EV1], and Generalised Logistic [GLO]) and assessing their goodness of fit with the Anderson-Darling test (Viglione, 2008). The Anderson-Darling test measures the extent of the departure, in terms of probabilities, between a simulated hypothetical distribution and the frequency

distribution for consideration. If the estimated probability is greater than some defined significance level, the test fails. Table 2 provides the percentage of cases when the goodness of fit failed at the 0.05 level of significance. Of the three distributions, the GEV provides the best fit to the annual maximum rainfalls, followed by the GLO and the Gumbel distribution. Both the GEV and GLO are three-parameter distributions allowing flexibility in fitting to data through the shape parameter.

Table 2. Percentage of sites, for the given frequency distributions and durations, failing the Anderson-Darling goodness of fit test at the p=0.05 level of significance

	10m	20m	30m	1h	2h	6h	12h	24h	48h	72h
GEV	8.7	8.0	8.1	5.9	7.8	7.5	6.6	4.8	4.6	5.2
GLO	13.1	9.5	13.7	10.2	9.8	8.4	8.0	8.1	8.2	10.0
EV1	19.0	17.1	17.0	17.1	14.1	11.0	6.4	10.5	7.7	7.5

The GEV is a flexible three-parameter distribution that combines three extreme-value distributions within a single framework: the Gumbel, Frechet and Weibull (Jenkinson, 1955). The parameters of the distribution are $\alpha > 0$, ξ and κ (i.e. scale, location and shape respectively) with a cumulative frequency distribution function given by

$$F(x) = \begin{cases} \exp(-1 - \kappa(x - \xi) / \alpha)^{1/\kappa} & \kappa \neq 0 \\ \exp(-\exp(-(x - \xi) / \alpha)) & \kappa = 0 \end{cases}$$

Here $\kappa < 0$ corresponds to a lower bound, heavy-tail Frechet distribution, $\kappa > 0$ to an upper bound light-tail Weibull distribution, and in the case of $\kappa = 0$ the Gumbel distribution is the limiting case as the shape parameter approaches zero. Two common methods of estimating the GEV parameters are method of maximum likelihood and the method of L-moments. Morrison and Smith (2002) proposed methods for estimating the GEV parameters that combine both maximum likelihood and L-moment methods. Subsequently, Ailliot et al, (2009) extended their method to include the asymptotic covariance structure of the estimates. Ailliot et al, (2009) parameter estimation method M1 is used here, where the shape parameter is determined using maximum likelihood, the scale and location parameters are estimated by L-moments. This is the MIX2 method in Morrison and Smith (2002), but subject to an additional constraint of $-0.5 < \kappa < 0.5$. The Appendix provides additional details about the GEV and deriving the parameter estimators.

Although κ is estimated using the mixed L-moment and maximum likelihood M1 method (Ailliot et al, 2009), the subsequent mapping of the frequency distribution parameters involved determining L-moment ratios τ and τ_3 (see Appendix for details). An L-moment equivalent for τ_3 can be determined directly from the following relation $\frac{2(1 - 3^{-k})}{1 - 2^{-k}} - 3$ (Hosking, 1990).

Data aspects

Parameters of the GEV distribution were fitted to data for each of the 10 durations at each site, provided there was at least 12 years of annual maximum rainfalls for the sub-daily durations, and 15 years for the daily durations. This reflects the relative lengths of the data where the record lengths of the annual maxima are generally smaller for sub-daily durations than for the longer durations. The minimum record lengths is also a compromise between fitting GEV distributions with small amounts of data which can lead to difficulties in estimating reliably the shape parameter (NERC, 1975; Lu and Stedinger, 1992; Rosbjerg and Madsen, 1995; Martins and Stedinger, 2000), and having a sufficiently large number of spatially distributed sites across New Zealand in order to produce acceptable nationwide maps of GEV parameters.

Frequency distributions, at a site, fitted to data from different durations are not always consistent. For example the 12-hour 100-year rainfall event could be smaller than the 6-hour 100-year rainfall. As a way to minimize this occurring, Durrans and Kirby (2004) proposed a three-class data typing based on the duration of storm rainfalls; daily, hourly, and sub-hourly. This also has a close meteorological equivalence of convective (sub-hourly) and synoptic (daily) storm typing reflecting the dominant dynamic atmospheric processes associated with such rainfalls (see also Thompson, 2002). The hourly data-type for durations from 2 – 12 hours is likely to be blend of both convective and synoptic scale processes as the storm dynamics transition from dominant convective processes to synoptic rainfall processes. Durrans and Kirby (2004) adjusted the L-moment ratios so that they would vary from site to site, but would remain constant across all durations with the given data-type, by computing averages of original L-moments for the constituent durations. To maintain consistency, the original second L-moment, λ_2 , and the corresponding ξ and α are adjusted to conform with the mean L- coefficient of variation, τ_2 , for the data-type.

Regional frequency analysis

Region of influence: Regional frequency analysis is a common method used in the estimation of quantiles when rainfall or river flow records are too short to allow reliable estimation of long recurrence intervals. Although regionalization was initially based on forming geographically contiguous regions, Acreman and Wiltshire (1989) suggested a regionalization that dispensed with fixed regions. This was taken up by Burn (1990) who developed the idea further into the region of influence approach. A region of influence is a site-specific region with a collection of sites with similar extreme rainfall properties that can be used in the estimation of quantiles at the site of interest. The collection of sites should be able to form a homogeneous region, and ideally the site of interest should be close to the centre of the group of sites as determined by an appropriate similarity measure (Burn, 1997). Robson and Reed (1999) advocated the use of pooling-groups, but the two terms are equivalent.

In determining a region of influence the number of sites included for membership was initially set at 25 (Burn, 1997), provided there were at least 5 times as many

station-years of annual maxima as the recurrence interval (Robson and Reed, 1997). Hosking and Wallis (1997) also commented that 20 sites was the optimum number of sites as more sites resulted in diminishing returns unless extreme quantiles are to be estimated. The 5T criterion (Robson and Reed, 1997) is a *rule of thumb*, but Cluckie and Pessoa (1990) noted that at least of 300 station-years of data provided relatively stable quantiles. Large data sets tended to be less affected by additional data (Hosking and Wallis, 1988).

A key component, in identifying a region of influence for regional frequency analysis, is to assess the homogeneity of the group of selected sites. This is done by the method of “test-remove-re-evaluate”. If the region of influence is not homogeneous by the *homogeneity test*, the site that is most dissimilar, in terms of a similarity metric, is *removed*, and the revised region of influence is *re-evaluated* for homogeneity. The process is repeated until the region of influence is considered homogeneous or until there are no fewer than 4T station-years of data. For T = 100-year, this still corresponds to 400 station-years of annual maxima.

For sub-daily durations, where there are fewer sites in the network and shorter record lengths than daily data, the above criteria can be relaxed (Jakob et al., 2007). For each region of influence a 3T rule of thumb was adopted provided there were at least 15 sites, but the test-remove-re-evaluate procedure is otherwise the same.

By way of example, the region of influence and the sites used for a Palmerston North Airport target site (40.327°S, 175.616°E) following the above homogeneity analysis procedure is given in Figure 4. The figure shows a region of influence that crosses the nearby mountain ranges. Since the site data are standardized by the respective site medians, the orographic and other site influences are largely removed. A dimensionless rainfall growth curve remains that is a function of the shape parameter for the given frequency distribution. The selected sites all lie within 25 km of Palmerston North Airport.

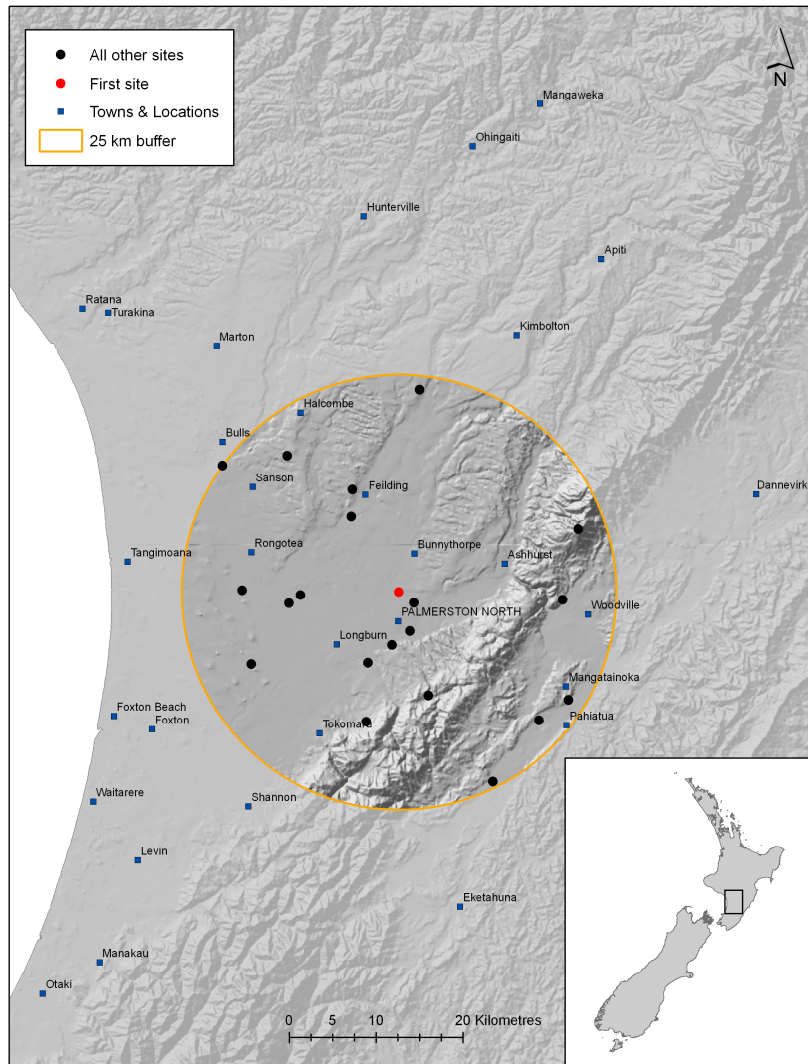


Figure 4. Sites selected in the region of influence surrounding Palmerston North Airport (red dot), following the test-remove re-evaluate homogeneity analysis. For reference purposes only, an orange circle with a 25km radius is included.

L-moment ratios for the region of influence are formed by a weighted-average of L-moment ratios from the individual sites where (Robson and Reed, 1997)

$$\tau_r^R = \frac{\sum_{i=1}^M w_i \tau_{ri}}{\sum_{i=1}^M w_i} \quad r=2, 3, 4 \text{ and } M \text{ is the number of sites in the region}$$

of influence, and w_i is an effective record length at site i , defined by $w_i = S_i n_i$. n_i is the actual record length and S_i is a similarity ranking factor (Robson and

Reed, 1997) given by $S_i = \frac{\sum_{j=i}^M n_j}{\sum_{j=1}^M n_j}$

Thus the most-similar site has a similarity ranking factor of 1, while at the M^{th} most-similar site $S_M = n_m / (n_1 + \dots + n_M)$.

For each of the 10 standard durations, regional L-moment ratios are computed. Following homogeneity testing (see section below) L-moment ratios for each data-type are subsequently formed using the approach given in an earlier paragraph.

Homogeneity testing: A starting point to test the homogeneity of a group of sites within a region of influence is the selection of a similarity metric defining the closeness of each site to every other site or group average. Any set of attributes in the similarity metric should not only be related to the extreme rainfall response at the target site, but should be easily obtainable from the available data that comprises the annual maximum rainfall series from all sites (Burn, 1990). The correlation between a 50-year rainfall event (actually the 50-year rainfall growth curve) and a set of candidate attributes (coefficient of variation, skewness parameter², plotting position of the 10-year rainfall event, L-moments, L-moment ratios, and parameter combinations from a GEV distribution) were evaluated. The three selected attributes with largest correlations were the coefficient of variation, skewness parameter and plotting position with values of 0.921, 0.534, and 0.819 respectively. These three parameters are used to develop a similarity metric. Burn (1990) based his metric on Euclidean distance, but more recently (Hosking and Wallis, 1997; Cunderlik and Burn, 2006) incorporated the sampling variability from the attributes and candidate sites, in the form of a Mahalanobis distance, which takes into account not only the group-average of all the sites but also the covariance structure of the attributes.

The similarity metric identifies which sites which are dissimilar relative to the group. Those sites whose similarity score exceeds a value of 3 (the approximate 10 percent significance level in Hosking and Wallis (1997) discordancy test) are removed from further consideration in the homogeneity analysis.

Critical to the regional frequency analysis method is the selection of a method to form regions of influence and the subsequent assessment of those groups. The previous paragraphs deals with a method to form a region of influence and the paragraph which follow deals with the homogeneity and testing of the groups. Many authors have proposed homogeneity tests (see Viglione et al, 2007 for a list of authors), and although the Hosking and Wallis (1997) method, based on L-moments, is routinely used in regional frequency analysis, there have been few general studies to identify which homogeneity test is most superior. Viglione et al (2007) is one such study, in which they compare tests based on L-moment ratios with those based on distribution-free rank tests. They compared the Hosking and Wallis HW_1 statistic, which is based solely on the variability of the L-CV in the region of influence, against the k-sample Anderson-Darling rank test, which is based on comparing individual sites with regional empirical distributions. Significant heterogeneity in the Region of Influence is found in the case of the Anderson-Darling test by estimating the 0.05 level of significance by Monte Carlo simulations. In the case of the Hosking and Wallis test, which compares the

² The skewness parameter is $(\mu - R_{med})/\sigma$, where μ , R_{med} , and σ are the mean, the median and the standard deviation respectively of the annual maximum rainfall.

variability of L-moment ratios for the group of sites with the expected variability obtained from simulation, if $HW_1 \geq 2$ then the region of influence is “definitely homogeneous” (Hosking and Wallis, 1997).

Viglione et al’s (2007) analyses showed that the Hosking and Wallis test is more powerful when the annual maxima are slightly skewed (i.e. when the regional L-coefficient of skewness is smaller than 0.23), while the k-sample Anderson-Darling rank tests perform more credibly when the L-coefficient of skewness is large. Figure 5 provides a scatter-plot of τ_2^R and τ_3^R of New Zealand data for each data-type. The vertical line on the τ_2^R axis is the $\tau_2^R = 0.23$ value: to the left of this line the Hosking and Wallis HW_1 test is considered best, and to the right the bootstrapped Anderson-Darling test is used. For the vast majority of pooling groups, the Hosking and Wallis test was used to assess its homogeneity. Also shown in this figure are the limits of the GEV shape parameter in terms of τ_3^R as determined by the mixed L-moment maximum likelihood method, along with a horizontal line specifying when $\kappa = 0$. For most of New Zealand the GEV shape parameter has values of less than zero (i.e. an EV2 or Frechet distribution).

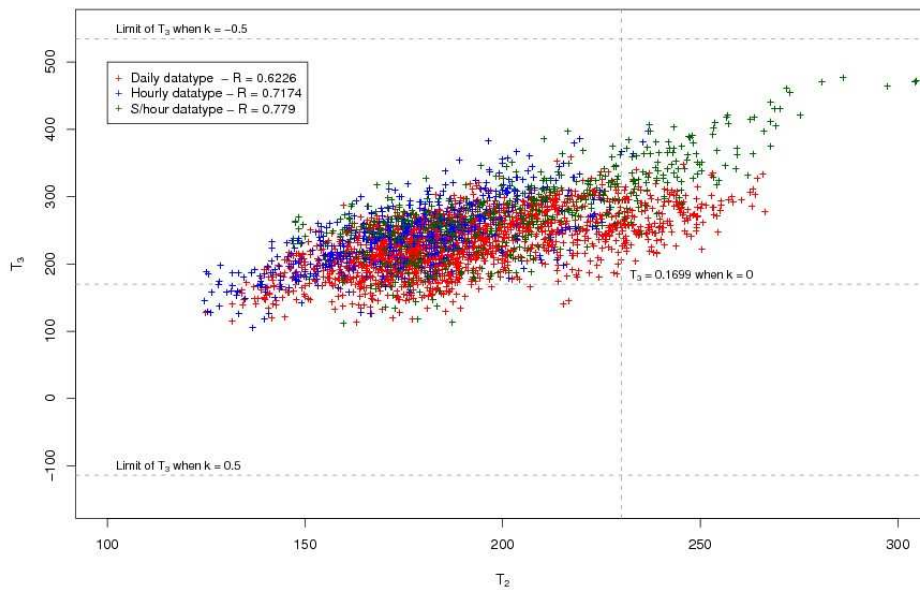


Figure 5. Scatter plot of L-coefficient of variation (τ_2) and L-coefficient of skewness (τ_3). The horizontal line at $\tau_2 = 0.23$ identifies the regions where the homogeneity tests are considered most powerful by Viglione et al (2007). The correlation between τ_2 and τ_3 are given in the diagram. Note the axes have been scaled up by 1000.

The homogeneity testing of New Zealand annual maximum rainfalls within the framework of a region of influence approach indicates several regions remaining heterogeneous (Table 3). As Lettenmaier et al (1987) and Hosking and Wallis (1988) and others have pointed out, regionalization of extreme rainfalls and river

flows are generally robust and relatively insensitive to some regional distributional heterogeneity.

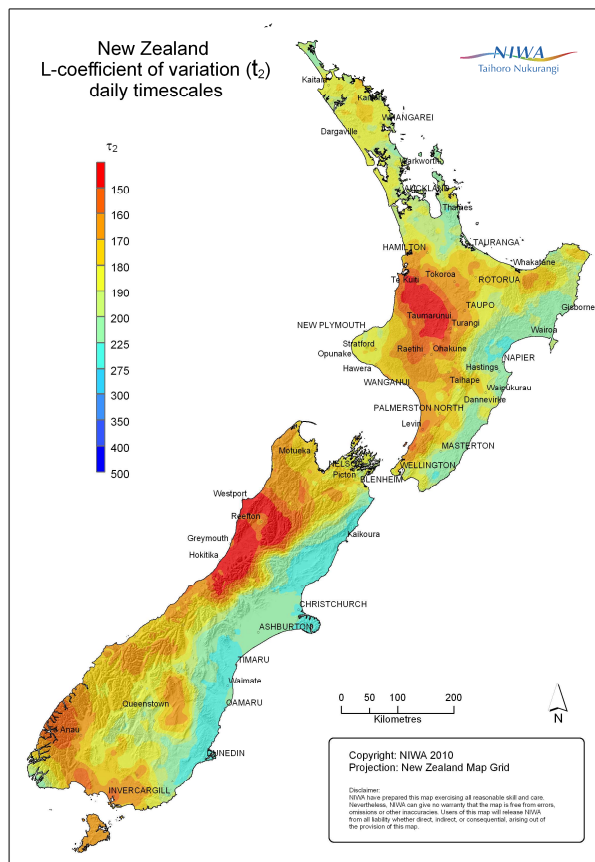
Table 3. Percentage of sites remaining heterogeneous following the Viglione homogeneity testing strategy.

Duration	10m	20m	30m	1h	2h	6h	12h	24h	48h	72h
%	15.1	11.1	9.7	2.8	4.4	1.9	1.2	2.0	1.9	2.6

Mapping the regional GEV parameters

Surfaces of regional L-coefficient of variation (τ_2^R) and L-coefficient of skewness (τ_3^R) for each of the data-types were fitted simultaneously using a common signal to error characteristic, and were mapped onto a 2km by 2km spot digital elevation model using the ANUSPLIN suite of programs. Maps of the spatial patterns for τ_2^R and τ_3^R for the daily data-type are given in Figure 6. Highest values of L-CV are generally in eastern regions of New Zealand and correspond to those areas of the country where the analogous coefficient of variation is also the largest. The smallest values of L-coefficient of skewness (i.e. where the shape parameter tends also to be close to zero or positive) tend to be, but not exclusively, in the western areas of New Zealand.

a. L-coefficient of skewness - τ_2^R



b. L-coefficient of skewness - τ_3^R

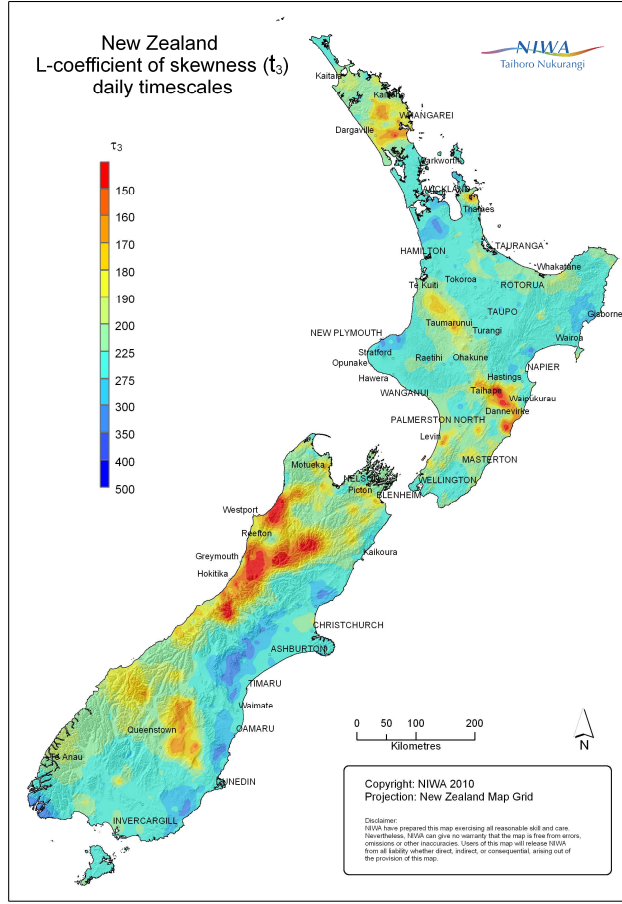


Figure 6. Spatial distribution of regional parameters of [a] τ_2^R and [b] τ_3^R of the GEV distribution for a daily data-type

Uncertainty in L-moment ratios: The variances and covariances of L-coefficient of variation and L-coefficient variation of skewness are

$$\text{Var}(\tau_2) = \text{Var}(\lambda_2 / \lambda_1) = \tau_2 (\text{Var}(\lambda_1) / \lambda_1^2 + \text{Var}(\lambda_2) / \lambda_2^2 - 2\text{Cov}(\lambda_1, \lambda_2) / \lambda_1 / \lambda_2)$$

$$\text{Var}(\tau_3) = \text{Var}(\lambda_3 / \lambda_2) = \tau_3 (\text{Var}(\lambda_2) / \lambda_2^2 + \text{Var}(\lambda_3) / \lambda_3^2 - 2\text{Cov}(\lambda_2, \lambda_3) / \lambda_2 / \lambda_3)$$

$$\text{Cov}(\tau_2, \tau_3) = \lambda_3 / \lambda_1^2 \lambda_2 \text{Cov}(\lambda_1 \lambda_2) - \text{Cov}(\lambda_1 \lambda_3) / \lambda_1^2 + \text{Cov}(\lambda_2 \lambda_3) / \lambda_1 \lambda_2 - \lambda_3 / \lambda_1 \lambda_2^2 \text{Var}(\lambda_2)$$

and are obtained by evaluating the unbiased distribution-free estimators of L-moments (Viglione, 2008). The variances and covariances of the sample regional L-moment ratios are given by Kjeldsen and Jones (2006) as

$$\text{Cov}(\tau_2^R, \tau_3^R) = \text{Cov} \left\{ \sum_{i=1}^M w_i \tau_{2i}, \sum_{i=1}^M w_i \tau_{3i} \right\}$$

where w_i are the similarity ranking factors (weights) at site i . Since the L-moment ratios are evaluated for three data-types (i.e. sub-hourly, hourly and daily durations), the variances and covariances are (assuming independence) are

simply the summation of the individual variances and covariances for each duration making up the data-type.

Other aspects in the development of HIRDS

Tables of T-year rainfall

Given the median annual maximum rainfall, R_{med} , and the two regional L-moment ratios τ_2^R and τ_3^R , T-year rainfall depths for a range of storm durations can be readily computed. The regional L-moment ratios derive the regional growth curve for a GEV frequency distribution. The shape parameter, κ , is computed directly from the L-coefficient of skewness, τ_3 , relationship in the Appendix, while the scale parameter is $\alpha = \beta / R_{med}$ and the location parameter $\xi = R_{med} (1 - \beta(1 - \log(2)^{\kappa}) / \kappa)$. The term β , given by Robson and Reed (1999), is $\beta = \kappa \tau_2 / (\tau_2 (\Gamma(1 + \kappa) - \log(2)^{\kappa}) + \Gamma(1 + \kappa)(1 - 0.5^{\kappa}))$.

When combined to provide quantiles (see the appropriate set of equations in the Appendix) a depth-duration-frequency (DDF) table or equivalently intensity-duration-frequency (IFD) table can be easily computed from the regional GEV parameter estimators. The upper most section of Figure 7 provides a depth-duration-frequency table for Kelburn, Wellington while the middle section provides a set of coefficients that can be used to generate the table (see below).

The covariance matrix of the parameters of the GEV distribution for the method of mixed L-moments and maximum likelihood is given by Ailliot et al. (2009). The variance of the quantile estimator $x(F)$ is obtained by the standard “delta method” $Var(x(F)) = B^T V B$, where V is the covariance matrix, and B^T is a vector given by $B^T = (\partial x(F) / \partial \xi, \partial x(F) / \partial \alpha, \partial x(F) / \partial \kappa)$. Standard errors are given by the square root of the variances, and these are displayed in the lowest section of Figure 7 for Kelburn, Wellington.

Consistency of design rainfall tables

In spite of using index-frequency method to estimate tables of depth-duration-frequency, it is all too common for the tables to remain internally inconsistent. If durations are treated separately, it is possible for “contradictions between rainfall events” (Faulkner, 1999) to occur between durations and recurrence intervals. Power laws of the form $R = aD^b$, where D is the duration, R is the rainfall depth or intensity and a and b are coefficients of the model, are commonly used to provide consistent tables. This was also done in the earlier version of HIRDS. Faulkner (1999) used a 6-coefficient flexible form of the power law relationship based on concatenated line segments. The model parameters define the DDF table in its entirety. The middle section of Figure 7 displays the table of coefficients for Kelburn, Wellington.

In this version of HIRDS, an 8-coefficient model is adopted to define the table of design rainfalls. It provides additional flexibility over a 6-coefficient model and the model takes the form given by

for $D \leq 1$ hour :

$$\ln(R) = (c_1 y + d_1) \ln(D) + ey + f$$

for $1 < D \leq 24$ hours :

$$\ln(R) = \ln(R_1) + (c_2 y + d_2) \ln(D)$$

for $D > 24$ hours :

$$\ln(R) = \ln(R_{24}) + (c_3 y + d_3) (\ln(D) - \ln(24))$$

where D is the duration in hours.

$$y = -\ln(-\ln(1-1/ARI))$$

A root mean squared error for fitting the model is computed, and this “error” is incorporated into the standard error associated with estimating the design rainfalls.

The intensity – frequency – duration table can be computed directly from the DDF table by simply dividing the rainfall depths by duration in hours. For the example given in Figure 7 a 30-minute 20-year rainfall depth at Kelburn is 21.9 mm. The equivalent rainfall intensity is 43.8 mm/h (i.e. 21.9 mm / 0.5 hours). Further, the rainfall intensity can also be obtained from the table of coefficients in the figure by applying the appropriate set of regression equations above, but with an additional coefficient to account for the reciprocal of the number of hourly units within the storm duration. The above equations become

for $D \leq 1$ hour :

$$\ln(R) = (c_1 y + d_1) \ln(D) + ey + f + \ln(h(D))$$

for $1 < D \leq 24$ hours :

$$\ln(R) = \ln(R_1) + (c_2 y + d_2) \ln(D) + \ln(h(D))$$

for $D > 24$ hours :

$$\ln(R) = \ln(R_{24}) + (c_3 y + d_3) (\ln(D) - \ln(24)) + \ln(h(D))$$

The values for $\ln(h(D))$ are given in Table 4.

Table 4. Coefficients to be applied to rainfall depth regression equations to obtain the equivalent rainfall intensity

Duration	10m	20m	30m	1h	2h	6h	12h	24h	48h	72h
h(D)	6	3	2	1	1/2	1/6	1/12	1/24	1/48	1/72
ln(h(D))	1.792	1.099	0.693	0.000	-0.693	-1.792	-2.485	-3.178	-3.871	-4.277

HIRDSV3 - High Intensity Rainfall Design System

Kelburn: Easting - 2658008 Northing - 5989891
 Generalised Extreme Value Distribution

11-Jan-2010

Rainfall depths (mm)		Duration									
ARI	aep	10m	20m	30m	60m	2h	6h	12h	24h	48h	72h
1.58	0.633	6.2	9.0	11.2	16.2	22.7	38.8	54.5	76.4	91.8	102.2
2.00	0.500	6.8	9.8	12.2	17.6	24.6	41.9	58.6	81.9	98.5	109.6
5.00	0.200	8.8	12.7	15.7	22.8	31.6	53.0	73.4	101.8	122.3	136.2
10.00	0.100	10.4	15.0	18.6	27.0	37.2	61.9	85.3	117.5	141.2	157.2
20.00	0.050	12.2	17.7	21.9	31.8	43.5	71.8	98.4	134.8	162.0	180.4
30.00	0.033	13.4	19.4	24.1	34.9	47.7	78.2	106.8	146.0	175.4	195.3
40.00	0.025	14.3	20.7	25.8	37.3	50.8	83.0	113.2	154.3	185.4	206.5
50.00	0.020	15.1	21.8	27.1	39.2	53.4	87.0	118.4	161.2	193.6	215.6
60.00	0.017	15.7	22.8	28.3	40.9	55.6	90.4	122.8	166.9	200.6	223.3
80.00	0.012	16.8	24.3	30.2	43.7	59.2	96.0	130.1	176.4	212.0	236.0
100.00	0.010	17.7	25.6	31.7	45.9	62.2	100.5	136.1	184.2	221.3	246.4

Coefficients							
c1	c2	c3	d1	d2	d3	e	f
0.0001	-0.011	0.0000	0.5330	0.4877	0.2650	0.2263	2.7861

Standard errors (mm)		Duration									
ARI	aep	10m	20m	30m	60m	2h	6h	12h	24h	48h	72h
1.58	0.633	0.4	0.4	0.5	0.5	0.6	0.8	1.0	1.1	1.3	1.4
2.00	0.500	0.4	0.4	0.5	0.5	0.6	0.9	1.1	1.2	1.5	1.6
5.00	0.200	0.5	0.5	0.6	0.7	0.8	1.4	1.8	1.9	2.3	2.4
10.00	0.100	0.6	0.7	0.8	1.1	1.2	2.0	2.7	2.7	3.3	3.6
20.00	0.050	0.7	1.0	1.2	1.6	1.7	3.0	4.0	4.0	5.0	5.3
30.00	0.033	0.9	1.2	1.5	2.1	2.2	3.8	5.0	5.1	6.2	6.7
40.00	0.025	1.0	1.4	1.8	2.4	2.5	4.4	5.9	5.9	7.3	7.8
50.00	0.020	1.1	1.6	2.0	2.8	2.8	4.9	6.6	6.6	8.1	8.7
60.00	0.017	1.2	1.8	2.2	3.1	3.1	5.4	7.2	7.3	8.9	9.6
80.00	0.012	1.4	2.0	2.6	3.6	3.6	6.3	8.3	8.3	10.2	11.0
100.00	0.010	1.6	2.3	2.9	4.0	4.0	7.0	9.3	9.3	11.4	12.2

Figure 7. Example of HIRDS output: Depth (mm) – duration (minutes or hours) – frequency (years) for Kelburn, Wellington. The upper-most table provides design rainfall estimates, the middle-table provides a set of coefficients with which to generate the DDF table, and the lower-most table gives estimates of the standard errors.

Site estimation of median annual maximum and L-moment ratios

From a practical application, the estimation of the index rainfall for any location in New Zealand is obtained from pooled estimates of the fitted value from the spline analysis, and, if available the actual site index-rainfall derived from the data. The pooled median takes the form (Kuzcera, 1983) $R_{med}^{pool} = sR_{med}^{site} + (1-s)R_{med}^{spline}$, where s provides the extent of each estimates influence on the pooled value. A similar procedure is also used for estimating the pooled L-moment ratios τ_2^R and τ_3^R .

Concluding Remarks

Estimates of high intensity rainfall for New Zealand have been revised and updated, and this report details the methods and techniques. A web-based application (<http://hirds.niwa.co.nz>) provides high intensity rainfall tables for New Zealand directly to the users PC.

Acknowledgements

This work was funded in part by the New Zealand Foundation for Research, Science and Technology. The following regional councils and unitary authorities provided valuable rainfall data for this project: Auckland Regional Council, Christchurch City Council, Environment Bay of Plenty, Environment Canterbury, Environment Southland, Environment Waikato, Gisborne District Council, Greater Wellington Regional Council, Hawkes Bay Regional Council, Horizons Regional Council, Marlborough Regional Council, Northland Regional Council, Otago Regional Council, Tasman District Council, Taranaki Regional Council, and West Coast Regional Council. Kathy Walter and Kevin McGill extracted extreme rainfalls from NIWA's nationally significant databases, and the maps were prepared by James Sturman. The efforts of the NIWA's System's Development Team in developing the web interface is gratefully acknowledged as are Ross Woods and Graeme Horrell in bringing the third version of HIRDS to completion.

Appendix. Additional notes on GEV distribution

The cumulative distribution function of a GEV with three parameters α , ξ and κ is

$$F(x) = \begin{cases} \exp(-1 - \kappa(x - \xi)/\alpha)^{1/\kappa} & \kappa \neq 0 \\ \exp(-\exp(-(x - \xi)/\alpha)) & \kappa = 0 \end{cases}$$

For $\kappa = 0$ the GEV distribution reduces to the Gumbel (EV1) distribution. The inverse functions of $F(x)$ above provide estimates of quantiles which are

$$x(F) = \begin{cases} \xi + \alpha(1 - (-\log(F(x)))^\kappa)/\kappa & \kappa \neq 0 \\ \xi - \alpha \log(\log(F(x))) & \kappa = 0 \end{cases}$$

The median of the GEV is found by substituting $F(x) = 0.5$ giving

$$R_{med} = \begin{cases} \xi + \alpha(1 - (\log(2))^\kappa)/\kappa & \kappa \neq 0 \\ \xi - \alpha(\log(\log(2))) & \kappa = 0 \end{cases}$$

Estimation of the parameters of a GEV using mixed methods follows Morrison and Smith (2002) and Ailliot et al., (2009). The log-likelihood of a GEV distribution for a random sample x_1, x_2, \dots, x_n is given by

$$\text{Log}(L) = -n \log(\alpha) - \sum_{i=1}^n y^{1/\kappa} + (1/\kappa - 1) \sum_{i=1}^n \log(y)$$

where $y = 1 - \kappa(x_i - \xi)/\alpha$, $i = 1, 2, \dots, n$. The corresponding maximum likelihood estimator are the values of α , ξ and κ that makes $\text{Log}(L)$ a maximum value. A feasible solution is subject to parameter constraints $\alpha > 0$ and $\kappa(x_i - \xi)/\alpha \leq 1$, $i = 1, 2, \dots, n$. It is further assumed that $-0.5 < \kappa < 0.5$. The inequality $\kappa < 0.5$ is required to satisfy conditions of maximum likelihood regularity (Smith, 1985), while $\kappa > -0.5$ ensures that data samples have finite second moments. These conditions on κ enables both L-moment and maximum likelihood estimation are consistent with asymptotic Gaussian distributions (Prescott and Walden, 1980, Hosking, 1990, Ailliot et al., 2009).

The first four L-moments of a GEV (Hosking, 1990) are

$$\begin{aligned} \lambda_1 &= \xi + \alpha(1 - \Gamma(1 + \kappa))/\alpha && (\text{mean}) \\ \lambda_2 &= \alpha(1 - 2^{-\kappa})\Gamma(1 + \kappa)/\kappa \\ \lambda_3/\lambda_2 &= \tau_3 = \frac{2(1 - 3^{-\kappa})}{1 - 2^{-\kappa}} - 3 && (L - \text{Skewness}) \\ \lambda_4/\lambda_2 &= \tau_4 = \frac{1 - 6(2^{-\kappa}) + 10(3^{-\kappa}) - 5(4^{-\kappa})}{1 - 2^{-\kappa}} && (L - \text{Kurtosis}) \end{aligned}$$

The last two L-moments are expressed as ratios. Another important L-moment ratio is $\tau_2 = \lambda_2/\lambda_1$, which is also the L-coefficient of variation (L-CV). L-moment ratios are analogous to conventional moment ratio estimates, such as the coefficients of variation and skewness.

For the mixed method M1 used in this study (the MIX2 method of Morrison and Smith, 2002), and estimate of κ is obtained by maximizing the above likelihood

function subject to the constraints noted above with α, ξ also constrained to be a solution of the first two L-moments (Ailliot et al., 2009).

References

Acreman, MC, Wiltshire, SE, 1989. The regions are dead; long live the regions: Methods for identifying and dispensing regions for flood frequency analysis, IAHS Publ., 187, 175-188.

Ailliot, P, Thompson, C, Thomson, P, 2009. Mixed methods for fitting the GEV distribution, Extremes, revised manuscript submitted, November 2009.

Austin, PM, Houze, RA Jr, 1970. Analysis of the structure of precipitation patterns in New England. J. Appl. Meteorol., 11, 926-934.

Beable, ME, McKerchar, AI, 1982. Regional flood estimation in New Zealand. Water & Soil Tech. Publ. 20. Ministry of Works and Development, Wellington, 139pp.

Burn, DH, 1990. Evaluation of regional flood frequency analysis with a region of influence approach, Water Resour. Res., 26, 10, 2257-2265.

Burn, DH, 1997. Catchment similarity for regional flood frequency analysis using seasonality measures, J. Hydrol, 202, 212-230.

Cluckie, ID, Pessoa, ML, 1990. Dam safety: an evaluation of some procedures for design flood estimation, Hydrol. Sci. J, 35, 5, 547-569.

Coulter, JD, Hessel, JWD, 1980. The frequency of high intensity rainfalls in New Zealand. Part II Point estimates. NZ Met. S. Misc Publ. 162, New Zealand Meteorological Service, Wellington, 76pp.

Cunane, C, 1989. Statistical distributions for flood frequency analysis. World Meteorological Organization, Operational Hydrology Report No 33, Geneva.

Cunderlik, JM and Burn DH, 2006. Switching the pooling similarity distances: Mahalanobis for Euclidean. Water Resources Research, 42, doi:10.1029/2005WRR004245, 2006.

Dalrymple, T, 1960. Flood-frequency analysis, US Geol. Surv. Water Supply Pap., 1543-A. US Govt. Printing Office, Washington DC.

de Haan, L, Ferreira, A, 2006. Extreme value theory: An introduction, 417pp, Springer, New York.

Durrans, SR, Kirby, JT, 2004. Regionalization of extreme precipitation estimates for the Alabama rainfall atlas. J. Hydrol., doi:10.1016/j.hydrol.2004.02.021

Faulkner, DS, 1999. Rainfall frequency estimation. Vol. 2, Flood Estimation Handbook, Institute of Hydrology, Wallingford.

Hosking, JRM, 1990. L-moments: analysis and estimation of distributions using linear combinations of order statistics. *J. Royal Stat. Soc. B52*, 105-124.

Hosking, JRM, Wallis, JR, 1988. The effect of intersite dependence on regional frequency analysis, *24*, 4, 588-600.

Hosking, JRM, Wallis, JR, 1997. *Regional frequency analysis: An approach based on L-moments*. Cambridge University Press, Cambridge, 224 pp.

Hutchinson, MF, 1995. Interpolating mean rainfall using thin plate smoothing splines. *Int. J. Geographical Information Systems*, 9, 385-403.

Hutchinson, MF, 1998. Interpolation of rainfall data with thin plate smoothing splines: II Analysis of topographic dependence. *J. Geographic Information and Decision Analysis*, 2, 168-185.

Hutchinson, MF, 2000. *ANUSPLIN Version 4.1 User Guide*. Centre for Resource and Environmental Studies. The Australian National University. Canberra.

Hutchinson, MF, Gessler, PE. (1994): Splines-more than just a smooth interpolator. *Geoderma*, 62, 45-67.

Jakob, D, Taylor, BF, Xuereb, K, 2005. A pilot study to explore methods for deriving design rainfalls for Australia. *Engineers Australia, 29th Hydrology and Water Resources Symposium*, Canberra, Australia.

Jakob, D, Xuereb, K, Taylor, BF, 2007. Revision of design rainfalls over Australia: A pilot study. *Aust. J. Water Resources*, 11(20) 153-159.

Jenkinson, AF, 1955. The frequency distribution of the annual maximum (or minimum) values of meteorological elements. *Q. J. Royal Meteor. Soc.*, 81, 158-171.

Katz, RW, Parlange, MB, Naveau, P, 2002. Statistics of extremes in hydrology, *Advances in Water Resources*, 25, 1287-1304.

Kendall, MG, Stuart, MA, 1977. *The Advanced Theory of Statistics*, vol 1, *Distribution Theory*, 4th ed., Griffin, London.

Kjeldsen, TR and Jones, DA, 2006. Prediction uncertainty in a median-based index flood method using L moments. *Water Resour. Res.*, 42, W07414, doi:10.1029/2005WR004069, 2006.

Kuzcera, G, 1983. Effect of sampling uncertainty and spatial correlation on an empirical Bayes procedure for combining site and regional information. *J. Hydrol.*, 65, 373-398.

Lettenmaier, DP, Wallis, JR and Wood, EF, 1987. Effect of regional heterogeneity on flood frequency estimation, *Water Resour. Res.*, 23, 313-323.

Lu L-H, and Stedinger, JR, 1992. Variance of two- and three-parameter GEV/PWM quantile estimators: formulae, confidence intervals, and a comparison, *J. Hydrol.*, 138, 247 – 267.

McKerchar, AI, Pearson, CPP, 1989. Flood frequency in New Zealand. Hydrology Centre Publ No. 20, Department of Scientific and Industrial Research, Christchurch, 87pp.

Nandakumar, N, Weinmann, E, Mein, RG, Nathan RJ, 1997. Estimation of extreme rainfalls for Victoria using the CRC-FORGE method. Report 97/4, Cooperative Research Centre for Catchment Hydrology, Monash University, 118pp.

Martins, ES, and Stedinger JR, 1995. Generalised maximum-likelihood generalised extreme value quantile estimators for hydrologic data, *Water Resour. Res.*, 36, 737 – 744.

Natural Environmental Research Council (NERC), 1975. Flood Studies Rep. Vol 1. NERC, London, 550 pp.

Prescott, P, Walden, AT, 1980. Maximum likelihood estimation of the parameters of the generalised extreme value distribution. *Biometrika*, 67, 723-724.

Robson, A, Reed, DW, 1999. Statistical procedures for flood frequency estimation, Vol 3, Flood Estimation Handbook, Institute of Hydrology, Wallingford.

Reed, DW, 1999. Overview, Vol 1, Flood Estimation Handbook, Institute of Hydrology, Wallingford.

Rosbjerg, D, and Madsen, H, 1995. Uncertainty measures of regional flood frequency estimators, *J. Hydrol.*, 167, 209 – 224.

Smith, RL, 1985. Maximum likelihood estimation in a class of non-regular cases. *Biometrika*, 72, 67-92.

Stewart, EJ, Reed, DW, Faulkner DS, Reynard, NS, 1999. The FORGEX method of rainfall growth estimation I: Review of requirement *Hydrology and Earth System Sciences*, 3, 187-195.

Thompson, CS, 1992. HIRDS (Manual and software). National Institute of Water and Atmospheric Research Ltd., Wellington, 20pp

Thompson, CS, 2002. The High Intensity Rainfall Design System: HIRDS. Proceedings International Conference on Flood Estimation, Berne, Switzerland. International Commission for the Hydrology of the Rhine Basin, CHR II-17, 273-282.

Tomlinson, AI, 1980. The frequency of high intensity rainfall. Part 1. Soil and Water Tech. Publ. No. 19. Ministry of Works and Development, Christchurch.

Viglione, A, 2008. Contributed R-Package: nsRFA (Non-supervised Regional Frequency Analysis). URL: <http://www.r-project.org/>

Viglione, A, Laio, F, Claps, P, 2007. A comparison of homogeneity tests for regional frequency analysis. Water Resources Research, 43, doi:10.1029/2006WR005095,.

Wallis, JR, Hosking JRM, 1997. Regional Frequency Analysis. An approach based on L-moments, 224pp, Cambridge University Press, Cambridge.

World Meteorological Organization (WMO), 1983. Guide to Hydrological Practices, vol. II, Analysis, forecasting, and other applications. WMO-No 168, 4th edition, Geneva.

Zheng, X, Basher, RE, 1995. Thin-plate smoothing spline modelling of spatial climate data and its application to mapping South Pacific rainfalls. Mon. Wea. Rev., 123. 3086-3102.